EUROPEAN LABORATORY FOR PARTICLE PHYSICS

CERN-EP/98-175
6th November 1998

A Measurement of the $\tau^- \rightarrow e^- \bar{\nu}_e \nu_\tau$ Branching Ratio

The OPAL Collaboration

Abstract

The branching ratio for the decay $\tau^- \rightarrow e^- \bar{\nu}_e \nu_\tau$ has been measured using Z^0 decay data collected by the OPAL experiment at LEP. In total 33 073 $\tau^- \rightarrow e^- \bar{\nu}_e \nu_\tau$ candidates were identified from a sample of 186 197 selected τ decays, giving a branching ratio of $B(\tau^- \rightarrow e^- \bar{\nu}_e \nu_\tau) = (17.81 \pm 0.09\ (\text{stat}) \pm 0.06\ (\text{syst}))\%$. This result is combined with other measurements to test e - μ and μ - τ universality in charged-current weak interactions. Additionally, the strong coupling constant $\alpha_s(m_\tau^2)$ has been extracted from $B(\tau^- \rightarrow e^- \bar{\nu}_e \nu_\tau)$ and evolved to the Z^0 mass scale, giving $\alpha_s(m_Z^2) = 0.1204 \pm 0.0011\ (\text{exp}) \pm 0.0019\ (\text{theory})$.

(Submitted to Physics Letters B)

The OPAL Collaboration

G. Abbiendi[2], K. Ackerstaff[8], G. Alexander[23], J. Allison[16], N. Altekamp[5], K.J. Anderson[9], S. Anderson[12], S. Arcelli[17], S. Asai[24], S.F. Ashby[1], D. Axen[29], G. Azuelos[18,a], A.H. Ball[17], E. Barberio[8], R.J. Barlow[16], R. Bartoldus[3], J.R. Batley[5], S. Baumann[3], J. Bechtluft[14], T. Behnke[27], K.W. Bell[20], G. Bella[23], A. Bellerive[9], S. Bentvelsen[8], S. Bethke[14], S. Betts[15], O. Biebel[14], A. Biguzzi[5], S.D. Bird[16], V. Blobel[27], I.J. Bloodworth[1], P. Bock[11], J. Böhme[14], D. Bonacorsi[2], M. Boutemeur[34], S. Braibant[8], P. Bright-Thomas[1], L. Brigliadori[2], R.M. Brown[20], H.J. Burckhart[8], P. Capiluppi[2], R.K. Carnegie[6], A.A. Carter[13], J.R. Carter[5], C.Y. Chang[17], D.G. Charlton[1,b], D. Chrisman[4], C. Ciocca[2], P.E.L. Clarke[15], E. Clay[15], I. Cohen[23], J.E. Conboy[15], O.C. Cooke[8], C. Couyoumtzelis[13], R.L. Coxe[9], M. Cuffiani[2], S. Dado[22], G.M. Dallavalle[2], R. Davis[30], S. De Jong[12], A. de Roeck[8], P. Dervan[15], K. Desch[8], B. Dienes[33,d], M.S. Dixit[7], J. Dubbert[34], E. Duchovni[26], G. Duckeck[34], I.P. Duerdoth[16], D. Eatough[16], P.G. Estabrooks[6], E. Etzion[23], F. Fabbri[2], M. Fanti[2], A.A. Faust[30], F. Fiedler[27], M. Fierro[2], I. Fleck[8], R. Folman[26], A. Fürtjes[8], D.I. Futyan[16], P. Gagnon[7], J.W. Gary[4], J. Gascon[18], S.M. Gascon-Shotkin[17], G. Gaycken[27], C. Geich-Gimbel[3], G. Giacomelli[2], P. Giacomelli[2], V. Gibson[5], W.R. Gibson[13], D.M. Gingrich[30,a], D. Glenzinski[9], J. Goldberg[22], W. Gorn[4], C. Grandi[2], K. Graham[28], E. Gross[26], J. Grunhaus[23], M. Gruwé[27], G.G. Hanson[12], M. Hansroul[8], M. Hapke[13], K. Harder[27], A. Harel[22], C.K. Hargrove[7], C. Hartmann[3], M. Hauschild[8], C.M. Hawkes[1], R. Hawkings[27], R.J. Hemingway[6], M. Herndon[17], G. Herten[10], R.D. Heuer[27], M.D. Hildreth[8], J.C. Hill[5], P.R. Hobson[25], M. Hoch[18], A. Hocker[9], K. Hoffman[8], R.J. Homer[1], A.K. Honma[28,a], D. Horváth[32,c], K.R. Hossain[30], R. Howard[29], P. Hüntemeyer[27], P. Igo-Kemenes[11], D.C. Imrie[25], K. Ishii[24], F.R. Jacob[20], A. Jawahery[17], H. Jeremie[18], M. Jimack[1], C.R. Jones[5], P. Jovanovic[1], T.R. Junk[6], D. Karlen[6], V. Kartvelishvili[16], K. Kawagoe[24], T. Kawamoto[24], P.I. Kayal[30], R.K. Keeler[28], R.G. Kellogg[17], B.W. Kennedy[20], D.H. Kim[19], A. Klier[26], S. Kluth[8], T. Kobayashi[24], M. Kobel[3,e], D.S. Koetke[6], T.P. Kokott[3], M. Kolrep[10], S. Komamiya[24], R.V. Kowalewski[28], T. Kress[4], P. Krieger[6], J. von Krogh[11], T. Kuhl[3], P. Kyberd[13], G.D. Lafferty[16], H. Landsman[22], D. Lanske[14], J. Lauber[15], S.R. Lautenschlager[31], I. Lawson[28], J.G. Layter[4], D. Lazic[22], A.M. Lee[31], D. Lellouch[26], J. Letts[12], L. Levinson[26], R. Liebisch[11], B. List[8], C. Littlewood[5], A.W. Lloyd[1], S.L. Lloyd[13], F.K. Loebinger[16], G.D. Long[28], M.J. Losty[7], J. Ludwig[10], D. Liu[12], A. Macchiolo[2], A. Macpherson[30], W. Mader[3], M. Mannelli[8], S. Marcellini[2], C. Markopoulos[13], A.J. Martin[13], J.P. Martin[18], G. Martinez[17], T. Mashimo[24], P. Mättig[26], W.J. McDonald[30], J. McKenna[29], E.A. Mckigney[15], T.J. McMahon[1], R.A. McPherson[28], F. Meijers[8], S. Menke[3], F.S. Merritt[9], H. Mes[7], J. Meyer[27], A. Michelini[2], S. Mihara[24], G. Mikenberg[26], D.J. Miller[15], R. Mir[26], W. Mohr[10], A. Montanari[2], T. Mori[24], K. Nagai[8], I. Nakamura[24], H.A. Neal[12], B. Nellen[3], R. Nisius[8], S.W. O'Neale[1], F.G. Oakham[7], F. Odorici[2], H.O. Ogren[12], M.J. Oreglia[9], S. Orito[24], J. Pálinkás[33,d], G. Pásztor[32], J.R. Pater[16], G.N. Patrick[20], J. Patt[10], R. Perez-Ochoa[8], S. Petzold[27], P. Pfeifenschneider[14], J.E. Pilcher[9], J. Pinfold[30], D.E. Plane[8], P. Poffenberger[28], J. Polok[8], M. Przybycień[8], C. Rembser[8], H. Rick[8], S. Robertson[28], S.A. Robins[22], N. Rodning[30], J.M. Roney[28], K. Roscoe[16], A.M. Rossi[2], Y. Rozen[22], K. Runge[10], O. Runolfsson[8], D.R. Rust[12], K. Sachs[10], T. Saeki[24], O. Sahr[34], W.M. Sang[25], E.K.G. Sarkisyan[23], C. Sbarra[29], A.D. Schaile[34], O. Schaile[34], F. Scharf[3], P. Scharff-Hansen[8], J. Schieck[11], B. Schmitt[8], S. Schmitt[11], A. Schöning[8], M. Schröder[8], M. Schumacher[3], C. Schwick[8], W.G. Scott[20], R. Seuster[14], T.G. Shears[8], B.C. Shen[4], C.H. Shepherd-Themistocleous[8], P. Sherwood[15], G.P. Siroli[2], A. Sittler[27], A. Skuja[17], A.M. Smith[8], G.A. Snow[17], R. Sobie[28], S. Söldner-Rembold[10], S. Spagnolo[20], M. Sproston[20], A. Stahl[3], K. Stephens[16], J. Steuerer[27], K. Stoll[10], D. Strom[19], R. Ströhmer[34], B. Surrow[8], S.D. Talbot[1], S. Tanaka[24], P. Taras[18], S. Tarem[22], R. Teuscher[8], M. Thiergen[10], J. Thomas[15], M.A. Thomson[8], E. von Törne[3], E. Torrence[8], S. Towers[6], I. Trigger[18], Z. Trócsányi[33], E. Tsur[23], A.S. Turcot[9], M.F. Turner-Watson[1], I. Ueda[24], R. Van Kooten[12], P. Vannerem[10], M. Verzocchi[10], H. Voss[3], F. Wäckerle[10], A. Wagner[27], C.P. Ward[5], D.R. Ward[5], P.M. Watkins[1], A.T. Watson[1], N.K. Watson[1], P.S. Wells[8], N. Wermes[3], J.S. White[6], G.W. Wilson[16], J.A. Wilson[1], T.R. Wyatt[16], S. Yamashita[24], G. Yekutieli[26], V. Zacek[18], D. Zer-Zion[8]

[1]School of Physics and Astronomy, University of Birmingham, Birmingham B15 2TT, UK
[2]Dipartimento di Fisica dell' Università di Bologna and INFN, I-40126 Bologna, Italy
[3]Physikalisches Institut, Universität Bonn, D-53115 Bonn, Germany
[4]Department of Physics, University of California, Riverside CA 92521, USA
[5]Cavendish Laboratory, Cambridge CB3 0HE, UK
[6]Ottawa-Carleton Institute for Physics, Department of Physics, Carleton University, Ottawa, Ontario K1S 5B6,

Canada
[7]Centre for Research in Particle Physics, Carleton University, Ottawa, Ontario K1S 5B6, Canada
[8]CERN, European Organisation for Particle Physics, CH-1211 Geneva 23, Switzerland
[9]Enrico Fermi Institute and Department of Physics, University of Chicago, Chicago IL 60637, USA
[10]Fakultät für Physik, Albert Ludwigs Universität, D-79104 Freiburg, Germany
[11]Physikalisches Institut, Universität Heidelberg, D-69120 Heidelberg, Germany
[12]Indiana University, Department of Physics, Swain Hall West 117, Bloomington IN 47405, USA
[13]Queen Mary and Westfield College, University of London, London E1 4NS, UK
[14]Technische Hochschule Aachen, III Physikalisches Institut, Sommerfeldstrasse 26-28, D-52056 Aachen, Germany
[15]University College London, London WC1E 6BT, UK
[16]Department of Physics, Schuster Laboratory, The University, Manchester M13 9PL, UK
[17]Department of Physics, University of Maryland, College Park, MD 20742, USA
[18]Laboratoire de Physique Nucléaire, Université de Montréal, Montréal, Quebec H3C 3J7, Canada
[19]University of Oregon, Department of Physics, Eugene OR 97403, USA
[20]CLRC Rutherford Appleton Laboratory, Chilton, Didcot, Oxfordshire OX11 0QX, UK
[22]Department of Physics, Technion-Israel Institute of Technology, Haifa 32000, Israel
[23]Department of Physics and Astronomy, Tel Aviv University, Tel Aviv 69978, Israel
[24]International Centre for Elementary Particle Physics and Department of Physics, University of Tokyo, Tokyo 113-0033, and Kobe University, Kobe 657-8501, Japan
[25]Institute of Physical and Environmental Sciences, Brunel University, Uxbridge, Middlesex UB8 3PH, UK
[26]Particle Physics Department, Weizmann Institute of Science, Rehovot 76100, Israel
[27]Universität Hamburg/DESY, II Institut für Experimental Physik, Notkestrasse 85, D-22607 Hamburg, Germany
[28]University of Victoria, Department of Physics, P O Box 3055, Victoria BC V8W 3P6, Canada
[29]University of British Columbia, Department of Physics, Vancouver BC V6T 1Z1, Canada
[30]University of Alberta, Department of Physics, Edmonton AB T6G 2J1, Canada
[31]Duke University, Dept of Physics, Durham, NC 27708-0305, USA
[32]Research Institute for Particle and Nuclear Physics, H-1525 Budapest, P O Box 49, Hungary
[33]Institute of Nuclear Research, H-4001 Debrecen, P O Box 51, Hungary
[34]Ludwigs-Maximilians-Universität München, Sektion Physik, Am Coulombwall 1, D-85748 Garching, Germany

[a] and at TRIUMF, Vancouver, Canada V6T 2A3
[b] and Royal Society University Research Fellow
[c] and Institute of Nuclear Research, Debrecen, Hungary
[d] and Department of Experimental Physics, Lajos Kossuth University, Debrecen, Hungary
[e] on leave of absence from the University of Freiburg

1 Introduction

Decays of τ leptons probe the Standard Model in both the electroweak and strong sectors. The leptonic branching ratios, in conjunction with τ lifetime and mass measurements, can be used to test the universality of charged-current couplings to electrons, muons and τ leptons [1]. In addition, large QCD corrections to the τ decay width enable the strong coupling constant α_s to be determined at the τ mass scale from a measurement of the $\tau^- \to \mathrm{e}^-\bar{\nu}_\mathrm{e}\nu_\tau$ branching ratio [1, 2].

This paper presents a measurement of the $\tau^- \to \mathrm{e}^-\bar{\nu}_\mathrm{e}\nu_\tau$ branching ratio[1] using data collected by the OPAL experiment [3] at energies near the Z^0 resonance. This measurement uses a larger data set than earlier OPAL measurements of $\mathrm{B}(\tau^- \to \mathrm{e}^-\bar{\nu}_\mathrm{e}\nu_\tau)$ [4, 5] and is based on a likelihood selection procedure. Tests of e - μ and μ - τ universality are presented and a value of $\alpha_s(m_\tau^2)$ is extracted from the branching ratio result within the context of fixed-order perturbation theory and evolved to the Z^0 mass.

2 Selection of τ jets

The OPAL experiment collected data corresponding to approximately 170 pb^{-1} of integrated luminosity during the period in which the LEP collider operated at centre-of-mass energies close to the Z^0 mass. Approximately 90% of these data were collected at the Z^0 peak and the remainder at energies within about 2 GeV of the peak. Candidate τ events used in this analysis are selected from this data set using a procedure similar to that described in previous OPAL publications [6].

Selection efficiencies and kinematic variable distributions were modelled using Monte Carlo simulated $\tau^+\tau^-$ event samples generated with the KORALZ 4.02 [7] package and the TAUOLA 2.0 [8] library. These events were then passed through a full simulation of the OPAL detector [9]. Events generated at energies approximately 2 GeV above and below the Z^0 peak were combined with the events generated on-peak in proportion to the integrated luminosities of the data. Background contributions from non-τ sources were evaluated using Monte Carlo samples based on the following generators: Multihadronic events ($\mathrm{e}^+\mathrm{e}^- \to \mathrm{q}\bar{\mathrm{q}}$) were simulated using JETSET 7.4 [10], $\mathrm{e}^+\mathrm{e}^- \to \mu^+\mu^-$ events using KORALZ [7], Bhabha events using BABAMC [11] and BHWIDE [12], and four fermion events using VERMASEREN 1.01 [13] and FERMISV [14].

At LEP, Z^0 bosons decaying at rest in the laboratory frame produce back-to-back τ pairs. Each highly-relativistic τ subsequently decays in flight, producing strongly collimated jets. Events selected as $\tau^+\tau^-$ are required to have exactly two such jets identified using a cone algorithm [15] with a cone half-angle of 35°. The average $|\cos\theta|$ of the two jets is required to be in the central region ($\overline{|\cos\theta|} < 0.68$) of the OPAL detector[2]. The scalar sum of the momenta of all tracks, p_tot, and the sum of the energies of all electromagnetic calorimeter (ECAL) clusters, E_tot, are required to satisfy $E_\mathrm{vis} \equiv E_\mathrm{tot} + p_\mathrm{tot} > 0.01 \cdot E_\mathrm{cm}$, where E_cm is the centre-of-mass energy, in order to be considered a good event. Backgrounds from cosmic rays are reduced to a negligible level by requirements on the time-of-flight detector. Two-photon mediated four-fermion events, $\mathrm{e}^+\mathrm{e}^- \to (\mathrm{e}^+\mathrm{e}^-)\mathrm{l}^+\mathrm{l}^-$ where $\mathrm{l}^+\mathrm{l}^-$ represents lepton pairs, are rejected by requirements on the acollinearity angle θ_acol, defined as the supplement of the angle between the two jets, and on the total energy and momentum of tracks and clusters in the event. The remaining background from two-photon mediated events was evaluated by comparing the θ_acol distribution in data and simulation, and was estimated to be $(0.21 \pm 0.02)\%$.

Decays of Z^0 bosons into lepton pairs produce low track and ECAL cluster multiplicities compared with multihadronic events ($\mathrm{e}^+\mathrm{e}^- \to \mathrm{q}\bar{\mathrm{q}}$). The $\tau^+\tau^-$ candidates are required to possess between two and six tracks and no more than ten ECAL clusters. Jets produced in multihadronic events are typically less collimated than those resulting from τ decays. The residual $\mathrm{e}^+\mathrm{e}^- \to \mathrm{q}\bar{\mathrm{q}}$ background was therefore evaluated by examining the collimation of tracks in the jets and was estimated to be $(0.38 \pm 0.05)\%$

Events within this low-multiplicity sample are expected to be lepton pairs, and are classified as either $\mathrm{e}^+\mathrm{e}^-$,

[1] Charge conjugation is assumed throughout this paper.

[2] In the OPAL coordinate system the e^- beam direction defines the $+z$ axis, and the centre of the LEP ring defines the $+x$ axis. The polar angle θ is measured from the $+z$ axis, and the azimuthal angle ϕ is measured from the $+x$ axis

Source	τ candidate sample (%)	$\tau^- \to e^- \bar{\nu}_e \nu_\tau$ sample (%)
$e^+e^- \to (e^+e^-)l^+l^-$	0.21 ± 0.02	0.62 ± 0.07
$e^+e^- \to q\bar{q}$	0.38 ± 0.05	0
$e^+e^- \to e^+e^-$	0.15 ± 0.03	0.67 ± 0.10
$e^+e^- \to \mu^+\mu^-$	0.52 ± 0.03	0
total	1.26 ± 0.07	1.29 ± 0.12

Table 1: Estimates of non-τ backgrounds in the τ candidate sample and in the $\tau^- \to e^- \bar{\nu}_e \nu_\tau$ candidate sample.

$\mu^+\mu^-$ or $\tau^+\tau^-$ based on tracking, calorimetry and muon chamber information. Bhabha events ($e^+e^- \to e^+e^-$) typically possess two high-momentum tracks and ECAL energy close to the full centre-of-mass energy. These events are rejected by requiring $E_{\rm tot} + 0.3 \cdot p_{\rm tot} \leq E_{\rm cm}$ and $E_{\rm vis} \leq 1.4 \cdot E_{\rm cm}$. The residual Bhabha background in the τ sample was determined to be $(0.15 \pm 0.03)\%$ by examining the distribution of $E_{\rm tot} + 0.3 \cdot p_{\rm tot}$ in events containing an electron.

Muon-pair events ($e^+e^- \to \mu^+\mu^-$) are characterized by two back-to-back high-momentum tracks associated with activity in the muon chambers or the hadron calorimeter and with little energy in the ECAL. Events with $E_{\rm vis} > 0.6 \cdot E_{\rm cm}$ in combination with a muon tag [6] in both jets are rejected. Muon-pair events which survive this cut generally do so because one of the muons has passed through a region of the detector which lacks muon chamber coverage. The background due to muon pairs was evaluated by examining the $E_{\rm vis}$ distribution of events with a single track in each jet, and was estimated to be $(0.52 \pm 0.03)\%$.

Fiducial cuts are imposed on the individual τ candidate jets to avoid regions of the detector associated with small gaps between structural units of the ECAL and to reject tracks which are close to the anode planes of the central jet chamber. Particles associated with these detector regions possess degraded ECAL energy and track momentum resolution respectively, resulting in a reduced ability to distinguish $\tau^- \to e^- \bar{\nu}_e \nu_\tau$ decays from other τ decays.

A total of 186 197 τ candidate jets pass the selection described above. Estimates of non-τ backgrounds in the τ candidate sample are summarized in table 1. In cases where the data are well described by the Monte Carlo distributions the uncertainties are determined by the statistical error in the distributions, otherwise the uncertainties have been increased to reflect the level of disagreement between the data and the simulated distributions. The total non-τ background was estimated to be $f_\tau = (1.26 \pm 0.07)\%$. The contribution from s-channel four-fermion final states was found to be negligible for all processes except for $e^+e^- \to e^+e^-\tau^+\tau^-$ which contributes at the level of $\sim 0.2\%$. However, the τ leptons produced in this process are added to the signal without introducing any significant measurement bias.

3 $\tau^- \to e^- \bar{\nu}_e \nu_\tau$ preselection

A $\tau^- \to e^- \bar{\nu}_e \nu_\tau$ decay in the OPAL detector typically consists of a single track in the jet chamber, associated with a single ECAL cluster having essentially the full energy of the decay electron. These decays are identified from the τ-sample using a cut-based preselection followed by a likelihood selection. The preselection consists of a collection of loose selection cuts which reject τ jets which are clearly inconsistent with $\tau^- \to e^- \bar{\nu}_e \nu_\tau$ decays. The preselection requirements are described in the remainder of this section.

The kinematic variables used in this selection are based primarily on tracking and calorimetry. Monte Carlo modelling of the selection variables was checked over the entire momentum range using selected data samples of τ decays. Additional verification of variable distributions for electrons was performed at high and low momenta using Bhabha and $e^+e^- \to (e^+e^-)e^+e^-$ data samples respectively (see Section 5). Several of the kinematic variables used in this analysis are "normalized" in order to remove the momentum dependence for $\tau^- \to e^- \bar{\nu}_e \nu_\tau$ decays. For a variable $K(p)$, the mean, $\mu_K(p)$, and width, $\sigma_K(p)$, are parameterized for $\tau^- \to e^- \bar{\nu}_e \nu_\tau$ decays

as a function of the track momentum p. The normalized quantity $N(K)$, defined as

$$N(K) \equiv \frac{K(p) - \mu_K(p)}{\sigma_K(p)} \quad , \tag{1}$$

has a distribution which is centred at zero and with a width of unity.

Although most $\tau^- \to e^-\bar{\nu}_e\nu_\tau$ decays produce only a single track in the jet chamber, in approximately 2% of these decays a radiated photon converts to an e^+e^- pair, producing additional tracks which may or may not be associated with distinct ECAL clusters. In order to allow for these photon conversions, the preselection accepts jets with up to three tracks. If more than one track is present in a jet, the highest momentum track is assumed to be the decay electron and is referred to as the primary track. The number of tracks in the jet ($N_{\rm tracks}$) is plotted in Figure 1a for τ jets which pass all other preselection requirements.

All $\tau^- \to e^-\bar{\nu}_e\nu_\tau$ candidate jets which have primary track momentum $p \geq 5$ GeV are required to have exactly one ECAL cluster associated to the track. Jets with $p < 5$ GeV are accepted even if the primary track has no associated cluster. ECAL clusters which are not associated to tracks, referred to as neutral clusters, may be produced either by radiated photons or by photons from π^0 decays. Jets containing up to two neutral clusters are accepted by the preselection. The number of neutral clusters ($N_{\rm neut}$) is plotted in Figure 1b.

The electromagnetic shower produced by the electron from a $\tau^- \to e^-\bar{\nu}_e\nu_\tau$ decay is normally fully contained in the ECAL and little or no activity is expected in the hadron calorimeter (HCAL). The depth of penetration of τ decay products into the HCAL is measured using the number of sequential HCAL layers, $N_{\rm HCAL}$, with activity associated with the τ candidate jet. Jets with $N_{\rm HCAL} > 3$ are rejected. This variable is plotted in Figure 1c. The discrepancy between data and Monte Carlo in this plot is due to the modelling of τ hadronic decays rather than $\tau^- \to e^-\bar{\nu}_e\nu_\tau$ decays, and its effect on the estimated background is understood.

The ratio of the energy of the associated ECAL cluster (E) to the momentum of the primary track (p) is typically near unity for $\tau^- \to e^-\bar{\nu}_e\nu_\tau$ decays, and less than one for other τ decays. This ratio is normalized as described above to create the selection variable $N(E/p)$ shown in Figure 2a. A preselection cut of $N(E/p) > -6.0$ is applied to all τ candidate jets which have an ECAL cluster associated with the primary track.

The ionization energy deposition ($\mathrm{d}E/\mathrm{d}x$) [16] of a charged particle traversing the central jet chamber is considered to be well measured if more than 20 out of a possible 159 signal wires collect a measurable charge. This criterion is satisfied for approximately 99.7% of electrons produced in $\tau^- \to e^-\bar{\nu}_e\nu_\tau$ decays. The normalized quantity $N(\mathrm{d}E/\mathrm{d}x)$ is constructed for all tracks with well measured $\mathrm{d}E/\mathrm{d}x$. Candidate jets in which the primary track possesses a well measured $\mathrm{d}E/\mathrm{d}x$ and $N(\mathrm{d}E/\mathrm{d}x) \leq -3.5$ are rejected (see Figure 2b).

All tracks other than the primary track are required to have properties which are consistent with electrons produced by a photon conversion. The quadratic sum of $N(\mathrm{d}E/\mathrm{d}x)$ of conversion-candidate tracks with well measured $\mathrm{d}E/\mathrm{d}x$ is required to be less than 2.5. The second highest momentum track in the jet is required to have momentum less than 4.0 GeV. If the jet contains three tracks, then the scalar sum of the momenta of the second and third tracks must be less than 6.0 GeV.

The preselection cuts described above reduce the background from hadronic τ decays to approximately 16% of the sample and the background from $\tau^- \to \mu^-\bar{\nu}_\mu\nu_\tau$ decays to a negligible level while maintaining a high efficiency (over 99%) for $\tau^- \to e^-\bar{\nu}_e\nu_\tau$ decays. The main $\tau^- \to e^-\bar{\nu}_e\nu_\tau$ selection is then accomplished by applying a likelihood selection to this sample, further reducing the τ background to the level of $\sim 1\%$.

4 $\tau^- \to e^-\bar{\nu}_e\nu_\tau$ likelihood selection

The sample of τ decays which survive the preselection requirements described above is used as the basis for a $\tau^- \to e^-\bar{\nu}_e\nu_\tau$ likelihood selection. For this selection, the Bayesian posterior probability $P(e|X)$ that an event represents a $\tau^- \to e^-\bar{\nu}_e\nu_\tau$ decay is estimated given measurements of a set X of uncorrelated kinematic variables. The $\tau^- \to e^-\bar{\nu}_e\nu_\tau$ selection is accomplished by applying a cut on the estimator $P(e|X)$. Jets which survive the

preselection can be classified as either $\tau^- \to e^- \bar{\nu}_e \nu_\tau$ decays or $\tau^- \to \pi^- (\geq 0\pi^0)\nu_\tau$ decays, so likelihood functions are constructed only for these two types of decays. The likelihood functions are based on reference histograms obtained from Monte Carlo simulation of a set of six selection variables.

The first two likelihood selection variables, $N(\Delta\theta)$ and $N(\Delta\phi)$, are normalized measures of the difference between the θ and ϕ position at which a charged particle enters the ECAL, as determined by tracking in the jet chamber, and the centroid of the associated ECAL cluster. Fluctuations in ECAL energy deposition by hadrons result in large variations in the reconstructed cluster position (~ 9 mrad) compared with the variations produced by electrons or photons (1 - 2 mrad). This difference in position resolution is used to discriminate between $\tau^- \to e^- \bar{\nu}_e \nu_\tau$ decays and hadronic τ decays, as shown in Figure 2c and 2d.

The remaining four likelihood selection variables, $N_{\rm neut}$, $N_{\rm HCAL}$, $N({\rm d}E/{\rm d}x)$ and $N(E/p)$, were described in the previous section. Jets which do not possess measurements of all likelihood selection variables are not automatically rejected. Instead, the likelihood is computed using the remaining variables. This can occur, for example, if a track with $p \leq 5$ GeV does not have an associated cluster so that no measurement of $N(E/p)$ is possible. The use of normalized variables implies that the selection variable reference distributions for $\tau^- \to e^- \bar{\nu}_e \nu_\tau$ decays are effectively independent of the track momentum. The background $\tau^- \to \pi^- (\geq 0\pi^0)\nu_\tau$ reference distributions, however, remain momentum dependent. Reference histograms are therefore constructed in the three momentum bins $p \leq 5$ GeV, $5 < p \leq 20$ GeV and $p > 20$ GeV.

The probability estimator $P(e|X)$ is plotted in Figure 3 for all τ jets which survive the preselection requirements. The likelihood selection cut of $P(e|X) > 0.35$ is optimized so as to minimize the total measurement uncertainty, and selects 33 073 $\tau^- \to e^- \bar{\nu}_e \nu_\tau$ candidates out of the sample of τ jets. The $\tau^- \to e^- \bar{\nu}_e \nu_\tau$ selection efficiency and the background due to τ other decays were estimated from τ Monte Carlo to be $(98.40 \pm 0.05)\%$ and $(1.21 \pm 0.04)\%$ respectively, where the quoted uncertainties are due to the Monte Carlo statistics only. The contributions to this background are $(0.48 \pm 0.03)\%$ from $\tau^- \to \pi^- \nu_\tau$, $(0.69 \pm 0.03)\%$ from $\tau^- \to \pi^- (\geq 1\pi^0)\nu_\tau$ and $(0.04 \pm 0.01)\%$ from other τ decays. Systematic uncertainties on the efficiency and background estimates are discussed in Section 5.

Non-τ events with electrons in the final state, such as $e^+e^- \to e^+e^-$ and $e^+e^- \to (e^+e^-)e^+e^-$, constitute a significant background in the $\tau^- \to e^- \bar{\nu}_e \nu_\tau$ candidate sample. These non-τ background contributions to the $\tau^- \to e^- \bar{\nu}_e \nu_\tau$ candidate sample were evaluated using the same methods as the corresponding backgrounds in the τ sample. Estimates of the contributions to this background are listed in Table 1 and total $f^{{\rm non}-\tau}_{\tau \to e\bar{\nu}\nu} = (1.29 \pm 0.12)\%$. The energy distribution of $\tau^- \to e^- \bar{\nu}_e \nu_\tau$ candidate jets is plotted in Figure 3.

5 Branching ratio results

The $\tau^- \to e^- \bar{\nu}_e \nu_\tau$ branching ratio is evaluated using the expression

$$ {\rm B}(\tau^- \to e^- \bar{\nu}_e \nu_\tau) = \left(\frac{N_e}{N_\tau} \right) \cdot \left(\frac{1 - f^\tau_{\tau \to e\bar{\nu}\nu} - f^{{\rm non}-\tau}_{\tau \to e\bar{\nu}\nu}}{(1 - f_\tau) \cdot \epsilon_e \cdot F_{\rm B}} \right) \quad , \tag{2} $$

where N_e and N_τ are the number of selected $\tau^- \to e^- \bar{\nu}_e \nu_\tau$ candidates and the number of τ candidate jets respectively, ϵ_e is the efficiency for selecting $\tau^- \to e^- \bar{\nu}_e \nu_\tau$ decays from the τ candidate sample and $f^\tau_{\tau \to e\bar{\nu}\nu}$ is the background in the $\tau^- \to e^- \bar{\nu}_e \nu_\tau$ sample due to τ decays. The fractional non-τ backgrounds in the τ candidate sample and in the $\tau^- \to e^- \bar{\nu}_e \nu_\tau$ candidate sample are given by f_τ and $f^{{\rm non}-\tau}_{\tau \to e\bar{\nu}\nu}$ respectively, and $F_{\rm B}$ is the τ selection bias factor which is discussed below. The values of these quantities are summarized in Table 2.

The τ selection procedure does not in general have a uniform efficiency for selecting different τ decay channels and therefore introduces a bias to the measured value of ${\rm B}(\tau^- \to e^- \bar{\nu}_e \nu_\tau)$. The τ selection bias factor $F_{\rm B}$ measures the degree to which the τ selection favours or suppresses the decay $\tau^- \to e^- \bar{\nu}_e \nu_\tau$ relative to other τ decay channels. It is defined as the ratio of the fraction of $\tau^- \to e^- \bar{\nu}_e \nu_\tau$ decays in a sample of τ decays after the τ selection is applied to the fraction before the selection. The bias factor was evaluated using a sample of approximately 1.1 million simulated $\tau^+\tau^-$ events. Systematic uncertainties on $F_{\rm B}$ were estimated by comparing data and Monte Carlo distributions of τ selection variables such as track and cluster multiplicities,

Quantity	Value
N_{e}	33 073
N_{τ}	186 197
F_{B}	1.0009 ± 0.0019
f_{τ}	$(1.26 \pm 0.07)\%$
$f^{\mathrm{non}-\tau}_{\tau\to \mathrm{e}\bar{\nu}\nu}$	$(1.29 \pm 0.12)\%$
ϵ_{e}	$(98.40 \pm 0.05)\%$
$f^{\tau}_{\tau\to \mathrm{e}\bar{\nu}\nu}$	$(1.21 \pm 0.04)\%$

Table 2: Values of quantities used in the calculation of $\mathrm{B}(\tau^- \to \mathrm{e}^-\bar{\nu}_{\mathrm{e}}\nu_{\tau})$. Note that the quoted uncertainties on ϵ_{e} and $f^{\tau}_{\tau\to \mathrm{e}\bar{\nu}\nu}$ are due to Monte Carlo statistics only.

and the ECAL energy scale. Monte Carlo variables were then smeared to cover the largest discrepancy between data and simulation and the observed shift in the measured bias factor was used as an estimate of the systematic uncertainty. Additional checks included modification of the cone finding algorithm and evaluation of the beam energy dependence of F_{B}. These studies result in a bias factor estimate of $F_{\mathrm{B}} = 1.0009 \pm 0.0019$, which contributes a systematic uncertainty of 0.034% to the branching ratio measurement.

The non-τ backgrounds $f^{\mathrm{non}-\tau}_{\tau\to \mathrm{e}\bar{\nu}\nu}$ and f_{τ} are correlated, since the background in the $\tau^- \to \mathrm{e}^-\bar{\nu}_{\mathrm{e}}\nu_{\tau}$ candidate sample also contributes to the background in the τ sample. A single systematic uncertainty of 0.025% is therefore assigned to the branching ratio measurement to account for the correlated uncertainties in the non-τ background estimates given in Table 2.

The systematic uncertainty due to Monte Carlo modelling of the likelihood selection variables was evaluated by varying the means and widths of the four normalized variables $N(\mathrm{d}E/\mathrm{d}x)$, $N(E/p)$, $N(\Delta\theta)$ and $N(\Delta\phi)$ around their central values and measuring the corresponding variation in the branching ratio result. The ranges of variation for each variable were estimated by comparing data and Monte Carlo distributions and were chosen to cover the largest discrepancies between data and simulation. The resulting shifts in the measured branching ratio were determined independently for each varied parameter and the uncertainty due to modelling of these variables was estimated by adding these shifts in quadrature. The contributions to this uncertainty from the modelling of the remaining two likelihood selection variables, N_{neut} and N_{HCAL}, were estimated by varying the preselection cuts on these quantities. The systematic uncertainty due to Monte Carlo modelling of the six likelihood selection variables was estimated to be 0.031%. The combined Monte Carlo statistical uncertainties on the efficiency and τ-background estimates given in Section 4 contribute an additional systematic uncertainty of 0.015% to the branching ratio measurement.

The preselection contributes to the branching ratio systematic uncertainty predominantly through the modelling of the preselection efficiency rather than the τ background. Modelling of preselection variables was verified with data by comparing the variable distributions of selected and rejected jets in samples in which all preselection cuts were applied other than the cut under consideration. All selection variables are well-modelled for $\tau^- \to \mathrm{e}^-\bar{\nu}_{\mathrm{e}}\nu_{\tau}$ decays. A systematic uncertainty of 0.015% was assigned due to the effect of preselection cuts which are not already covered by the selection variable modelling uncertainty or photon conversion uncertainties which are treated separately. The dominant contribution to this uncertainty is from the associated cluster requirement for tracks with $p \geq 5$ GeV.

The systematic uncertainty introduced by Monte Carlo modelling of photon conversions was evaluated by modifying the preselection cuts to reject jets possessing more than one track. This was found to introduce a shift of 0.005% to the measured branching ratio. Jets with up to three tracks were then re-admitted to the $\tau^- \to \mathrm{e}^-\bar{\nu}_{\mathrm{e}}\nu_{\tau}$ candidate sample but the momentum and $N(\mathrm{d}E/\mathrm{d}x)$ cuts on the second and third tracks were not applied. A significantly higher background and a slightly increased $\tau^- \to \mathrm{e}^-\bar{\nu}_{\mathrm{e}}\nu_{\tau}$ selection efficiency were obtained, and the reconstructed branching ratio was found to shift by 0.007%. A systematic uncertainty of 0.010% was assigned as a result of these tests.

The systematic uncertainty estimates from the effects discussed above are summarized in Table 3. Combining these values gives a total branching ratio systematic uncertainty of 0.057%. As a cross check, the likelihood selection cut was varied over the range $0.1 < P(e|X) < 0.8$ and the branching ratio result was evaluated at each

Source	Uncertainty (%)
Bias factor	0.034
Likelihood selection modelling	0.031
Non-τ backgrounds	0.025
Preselection	0.015
Monte Carlo statistics	0.015
Photon conversions	0.010
Total systematic uncertainty	0.057

Table 3: Contributions to the total branching ratio absolute systematic uncertainty.

value of this cut. The resulting variation of the branching ratio was found to be consistent with the estimated systematic uncertainties over the full range of likelihood cuts. Each of the six selection variables was then dropped in turn from the likelihood selection, and the posterior probability estimator was computed using the remaining five variables. A cut at 0.35 was imposed on each of these estimators and the six branching ratio measurements obtained in this manner were found to be consistent within the likelihood selection systematic uncertainty quoted above, indicating that no individual selection variable introduces a bias which exceeds the estimated uncertainty.

Modelling of selection variable distributions and the electron identification efficiency of the $\tau^- \to \mathrm{e}^-\bar{\nu}_\mathrm{e}\nu_\tau$ selection were checked over the accessible momentum range using data control samples of Bhabha and two-photon $\mathrm{e}^+\mathrm{e}^- \to (\mathrm{e}^+\mathrm{e}^-)\mathrm{e}^+\mathrm{e}^-$ events. A pure data sample of electron jets was obtained from Bhabha events by selecting low-multiplicity events with $E_\mathrm{tot} > 80$ GeV, $\theta_\mathrm{acol} < 0.75^\circ$ and requiring a tagged electron in the opposite jet. The full $\tau^- \to \mathrm{e}^-\bar{\nu}_\mathrm{e}\nu_\tau$ selection was then applied to this data sample and the efficiency was compared with that found using the Bhabha Monte Carlo simulation. A similar check was performed at low momentum using two-photon $\mathrm{e}^+\mathrm{e}^- \to (\mathrm{e}^+\mathrm{e}^-)\mathrm{e}^+\mathrm{e}^-$ events selected by requiring $\theta_\mathrm{acol} > 20^\circ$ and a tagged electron in the opposite jet. In both of these data samples the overall efficiencies were found to be consistent with the Monte Carlo simulation at the level of 0.06%.

Substituting the values from Table 2 into equation 2 and using the systematic uncertainty estimate above gives a branching ratio measurement of

$$\mathrm{B}(\tau^- \to \mathrm{e}^-\bar{\nu}_\mathrm{e}\nu_\tau) = (17.81 \pm 0.09\ (\mathrm{stat}) \pm 0.06\ (\mathrm{syst}))\,\% \quad . \tag{3}$$

This result is the most precise measurement of $\mathrm{B}(\tau^- \to \mathrm{e}^-\bar{\nu}_\mathrm{e}\nu_\tau)$ to date, and is in good agreement with other measurements of this quantity [17].

6 Lepton universality tests

In the Standard Model, the leptonic partial decay widths of the τ, including electroweak radiative corrections of order α and neglecting neutrino masses, are given by [18, 19]

$$\Gamma(\tau^- \to l^-\bar{\nu}_l\nu_\tau) = \frac{g_\tau^2 g_l^2}{(8m_\mathrm{W}^2)^2}\frac{m_\tau^5}{96\pi^3} f\left(\frac{m_l^2}{m_\tau^2}\right)(1+\delta_{RC}^\tau) \quad , \tag{4}$$

where m_l is the mass of the lepton ($l = \mathrm{e}, \mu$), m_τ is the mass of the τ lepton, m_W is the mass of the $\mathrm{W}^\pm$ boson and $f(x) = 1 - 8x + 8x^3 - x^4 - 12x^2\ln x$ is a phase-space correction factor. The term

$$(1+\delta_{RC}^\tau) = \left[1 + \frac{3m_\tau^2}{5m_\mathrm{W}^2}\right]\left[1 + \frac{\alpha(m_\tau^2)}{2\pi}\left(\frac{25}{4} - \pi^2\right)\right] \tag{5}$$

represents leading order $\mathrm{W}^\pm$ propagator and radiative corrections, where $\alpha(m_\tau^2) = 1/133.29$ is the fine structure constant at the τ mass scale. The coupling constants g_τ and g_l describe the strength of the coupling of the $\mathrm{W}^\pm$ to the different lepton generations. Lepton universality requires that g_e, g_μ and g_τ are identical.

The ratio of g_μ/g_e can be evaluated by comparing the τ decay widths to electrons and muons using equation 4, giving

$$\left(\frac{g_\mu}{g_\mathrm{e}}\right)^2 = \frac{\mathrm{B}(\tau^- \to \mu^- \bar{\nu}_\mu \nu_\tau)}{\mathrm{B}(\tau^- \to \mathrm{e}^- \bar{\nu}_\mathrm{e} \nu_\tau)} \frac{f(m_\mathrm{e}^2/m_\tau^2)}{f(m_\mu^2/m_\tau^2)} \quad . \tag{6}$$

The phase-space correction factors have the values $f(m_\mathrm{e}^2/m_\tau^2) = 1.0000$ and $f(m_\mu^2/m_\tau^2) = 0.9726$. Using the OPAL $\tau^- \to \mu^- \bar{\nu}_\mu \nu_\tau$ branching ratio measurement $(17.36 \pm 0.27)\%$ [5], one obtains $g_\mu/g_\mathrm{e} = 1.0011 \pm 0.0083$, in good agreement with the hypothesis of e - μ universality.

A test of μ - τ universality can be made by comparing the partial widths for $\tau^- \to \mathrm{e}^- \bar{\nu}_\mathrm{e} \nu_\tau$ and $\mu^- \to \mathrm{e}^- \bar{\nu}_\mathrm{e} \nu_\mu$ decays. The $\mu^- \to \mathrm{e}^- \bar{\nu}_\mathrm{e} \nu_\mu$ width is given by an expression equivalent to equation 4. The ratio of the couplings g_τ and g_μ is then given by

$$\frac{\Gamma(\tau^- \to \mathrm{e}^- \bar{\nu}_\mathrm{e} \nu_\tau)}{\Gamma(\mu^- \to \mathrm{e}^- \bar{\nu}_\mathrm{e} \nu_\mu)} = \frac{g_\tau^2 \, m_\tau^5 \, f\left(m_\mathrm{e}^2/m_\tau^2\right) (1 + \delta_{RC}^\tau)}{g_\mu^2 \, m_\mu^5 \, f\left(m_\mathrm{e}^2/m_\mu^2\right) (1 + \delta_{RC}^\mu)} \quad , \tag{7}$$

where $(1 + \delta_{RC}^\mu)$ represents the $\mathrm{W}^\pm$ propagator and radiative corrections to the $\mu^- \to \mathrm{e}^- \bar{\nu}_\mathrm{e} \nu_\mu$ width analogous to equation 5. Substituting numerical values for the correction factors gives

$$\left(\frac{g_\tau}{g_\mu}\right)^2 = 0.9996 \, \frac{\tau_\mu}{\tau_\tau} \frac{m_\mu^5}{m_\tau^5} \, \mathrm{B}(\tau^- \to \mathrm{e}^- \bar{\nu}_\mathrm{e} \nu_\tau) \quad . \tag{8}$$

Using the OPAL value for the τ lifetime, $\tau_\tau = 289.2 \pm 1.7 \pm 1.2$ fs [20], the BES Collaboration value for the τ mass, 1777.0 ± 0.3 MeV/c^2 [21], and Particle Data Group [17] values for the muon mass and lifetime, τ_μ, gives the result $g_\tau/g_\mu = 1.0025 \pm 0.0047$. The OPAL τ lifetime and $\mathrm{B}(\tau^- \to \mathrm{e}^- \bar{\nu}_\mathrm{e} \nu_\tau)$ are compared with the Standard Model prediction in Figure 4.

7 Measurement of α_s

A measurement of α_s can be extracted from the ratio R_τ of the hadronic decay width to the electronic decay width:

$$R_\tau \equiv \frac{\Gamma(\tau^- \to \text{ hadrons } \nu_\tau)}{\Gamma(\tau^- \to \mathrm{e}^- \bar{\nu}_\mathrm{e} \nu_\tau)} \quad . \tag{9}$$

Significant deviations from the parton level prediction $R_\tau \simeq 3$ can be accounted for in terms of QCD dynamics [22, 23, 24, 25] and are sufficiently large to allow a measurement of α_s. Perturbative and non-perturbative corrections to the parton level prediction can be organized in powers of $1/m_\tau^2$ using the short-distance Operator Product Expansion [26], giving

$$R_\tau = 3 \left(|V_\mathrm{ud}|^2 + |V_\mathrm{us}|^2\right) S_{EW} \left\{ 1 + \delta_{EW} + \delta^{(0)} + \sum_{D=2,4,\ldots} \delta^{(D)} \right\} \quad , \tag{10}$$

where $\delta^{(D)}$ are QCD condensates which are suppressed by $1/m_\tau^D$. The factors $S_{EW} = 1.0194 \pm 0.0040$ [19] and $\delta_{EW} = 0.0010$ [27] are electroweak corrections, and $V_\mathrm{ud} = 0.9753 \pm 0.0008$ and $V_\mathrm{us} = 0.2205 \pm 0.0018$ are CKM matrix elements [17]. Perturbative QCD corrections contribute at dimension $D = 0$ and have been calculated to be [23]

$$\delta^{(0)} = \left(\frac{\alpha_s(m_\tau^2)}{\pi}\right) + 5.2023 \left(\frac{\alpha_s(m_\tau^2)}{\pi}\right)^2 + 26.366 \left(\frac{\alpha_s(m_\tau^2)}{\pi}\right)^3 + \mathcal{O}({\alpha_s}^4) \quad . \tag{11}$$

The coefficient of the $\mathcal{O}({\alpha_s}^4)$ term is $(78.00 + K_4)$, where the K_4 coefficient has been estimated to be $K_4 \approx 25 \pm 50$ [25, 28]. The theoretical uncertainty in the perturbative expansion is taken to be due only to the K_4 uncertainty. Quark mass corrections contribute at dimension $D = 2$ and total $\delta^{(2)} = -0.010 \pm 0.002$. Non-perturbative QCD corrections enter at dimension $D \geq 4$ and have been estimated to total -0.010 ± 0.004 [24, 29]. Recent experimental measurements of the moments of the τ hadronic spectral functions have confirmed the size of these condensates [30, 31].

Source	Uncertainty	$\Delta\alpha_s(m_\tau^2)$	$\Delta\alpha_s(m_{\mathrm{Z}}^2)$
Scale dependence	$\mu^2/m_\tau^2 \to 0.4 - 2.0$	0.009	0.0009
RS dependence	$\overline{\mathrm{MS}} \to$ PMS	0.010	0.0011
K_4 dependence	$K_4 = 25 \pm 50$	0.006	0.0007
$\delta^{(D)}$ corrections ($D \geq 2$)	-0.020 ± 0.004	0.004	0.0005
Electroweak corrections	1.0194 ± 0.0040	0.004	0.0005
Running $\alpha_s(m_\tau^2) \to \alpha_s(m_{\mathrm{Z}}^2)$	-	-	0.0003
Total theory uncertainty	-	0.016	0.0019

Table 4: Theoretical uncertainties on $\alpha_s(m_\tau^2)$ and $\alpha_s(m_{\mathrm{Z}}^2)$.

Under the assumption of lepton universality, R_τ can be expressed in terms of the $\tau^- \to \mathrm{e}^-\bar{\nu}_\mathrm{e}\nu_\tau$ branching ratio only:

$$R_\tau = \frac{1 - \mathrm{B}(\tau^- \to \mathrm{e}^-\bar{\nu}_\mathrm{e}\nu_\tau) \cdot (1.9726)}{\mathrm{B}(\tau^- \to \mathrm{e}^-\bar{\nu}_\mathrm{e}\nu_\tau)} \quad , \tag{12}$$

where the numerical factor is from the phase space correction factor in Section 6. Substituting the branching ratio result from Section 5 gives the experimental value $R_\tau = 3.642 \pm 0.033$. A value of $\alpha_s(m_\tau^2)$ can be extracted from this result using equations 10 and 11, yielding

$$\alpha_s(m_\tau^2) = 0.334 \pm 0.010\ (\mathrm{exp}) \pm 0.016\ (\mathrm{theory}) \quad . \tag{13}$$

Contributions to the theoretical uncertainty, listed in Table 4, are dominated by the renormalization-scheme and scale dependences. The scale dependence is taken from [31], while the renormalization scheme dependence was estimated in [32] by evaluating the effect of changing from the $\overline{\mathrm{MS}}$ scheme to a scheme using the principle of minimal sensitivity (PMS).

The value of $\alpha_s(m_\tau^2)$ is evolved to the Z^0 mass scale for comparison with other measurements. The β coefficients of the renormalization group equations have recently been calculated up to four loops in the $\overline{\mathrm{MS}}$ scheme [33]. Following the procedure described in [34], running is performed at four loops, with three-loop matching conditions used to pass the heavy quark mass thresholds. This procedure has been shown to introduce an uncertainty of 0.0003 to the extracted value of $\alpha_s(m_{\mathrm{Z}}^2)$ [34]. Evolving the result from expression 13 gives

$$\alpha_s(m_{\mathrm{Z}}^2) = 0.1204 \pm 0.0011\ (\mathrm{exp}) \pm 0.0019\ (\mathrm{theory})\ , \tag{14}$$

which is in good agreement with determinations of $\alpha_s(m_{\mathrm{Z}}^2)$ using measurements at other energy scales [17].

8 Conclusions

Data collected by the OPAL experiment at energies near the Z^0 resonance have been used to determine the $\tau^- \to \mathrm{e}^-\bar{\nu}_\mathrm{e}\nu_\tau$ branching ratio. A total of 33 073 candidate $\tau^- \to \mathrm{e}^-\bar{\nu}_\mathrm{e}\nu_\tau$ decays were identified from a sample of 186 197 τ decays, using a likelihood-based selection, to give a branching ratio measurement of $\mathrm{B}(\tau^- \to \mathrm{e}^-\bar{\nu}_\mathrm{e}\nu_\tau) = (17.81 \pm 0.09\ (\mathrm{stat}) \pm 0.06\ (\mathrm{syst})\ )\%$. This result supersedes previous OPAL $\tau^- \to \mathrm{e}^-\bar{\nu}_\mathrm{e}\nu_\tau$ branching ratio measurements [4, 5] and is the most precise measurement of this quantity to date. This result has been combined with measurements of other quantities to test the universality of e - μ and μ - τ charged-current couplings to a precision of better than 1%. In addition, the strong coupling constant $\alpha_s(m_\tau^2)$ has been extracted from $\mathrm{B}(\tau^- \to \mathrm{e}^-\bar{\nu}_\mathrm{e}\nu_\tau)$ yielding $\alpha_s(m_\tau^2) = 0.334 \pm 0.010\ (\mathrm{exp}) \pm 0.016\ (\mathrm{theory})$. Evolving this value to the Z^0 mass scale gives $\alpha_s(m_{\mathrm{Z}}^2) = 0.1204 \pm 0.0011\ (\mathrm{exp}) \pm 0.0019\ (\mathrm{theory})$.

Acknowledgements

We particularly wish to thank the SL Division for the efficient operation of the LEP accelerator at all energies and for their continuing close cooperation with our experimental group. We thank our colleagues from CEA,

DAPNIA/SPP, CE-Saclay for their efforts over the years on the time-of-flight and trigger systems which we continue to use. In addition to the support staff at our own institutions we are pleased to acknowledge the
Department of Energy, USA,
National Science Foundation, USA,
Particle Physics and Astronomy Research Council, UK,
Natural Sciences and Engineering Research Council, Canada,
Israel Science Foundation, administered by the Israel Academy of Science and Humanities,
Minerva Gesellschaft,
Benoziyo Center for High Energy Physics,
Japanese Ministry of Education, Science and Culture (the Monbusho) and a grant under the Monbusho International Science Research Program,
Japanese Society for the Promotion of Science (JSPS),
German Israeli Bi-national Science Foundation (GIF),
Bundesministerium für Bildung, Wissenschaft, Forschung und Technologie, Germany,
National Research Council of Canada,
Research Corporation, USA,
Hungarian Foundation for Scientific Research, OTKA T-016660, T023793 and OTKA F-023259.

References

[1] A. Pich, Nucl. Phys. **55C** (Proc. Suppl.) (1997) 3.

[2] E. Braaten, Nucl. Phys. **55C** (Proc. Suppl.) (1997) 369.

[3] OPAL Collaboration, K. Ahmet *et al.*, Nucl. Inst. and Meth. **A305** (1991) 275; P.P. Allport *et al.*, Nucl. Inst. and Meth. **A346** (1994) 476; P.P. Allport *et al.*, Nucl. Inst. and Meth. **A324** (1993) 34; O. Biebel *et al.*, Nucl. Inst. and Meth. **A323** (1992) 169.

[4] OPAL Collaboration, G. Alexander *et al.*, Phys. Lett. **B369** (1996) 163.

[5] OPAL Collaboration, R. Akers *et al.*, Z. Phys. **C66** (1995) 543.

[6] OPAL Collaboration, G. Alexander *et al.*, Phys. Lett. **B266** (1991) 201;
OPAL Collaboration, P. Acton *et al.*, Phys. Lett. **B288** (1992) 373.

[7] KORALZ 4.0 generator: S. Jadach, B.F.L. Ward, and Z. Wąs, Comp. Phys. Comm. **79** (1994) 503.

[8] TAUOLA 2.0 generator: S. Jadach *et al.*, Comp. Phys. Comm. **76** (1993) 361.

[9] J. Allison *et al.*, Nucl. Inst. and Meth. **A317** (1992) 47.

[10] JETSET 7.4 generator: Sjöstrand, Comp. Phys. Comm. **82** (1994) 74.

[11] BABAMC generator: F.A. Berends, R. Kleiss and W. Hollik, Nucl. Phys. **B304** (1988) 712.

[12] BHWIDE generator: S. Jadach, W. Placzek and B.F.L. Ward, Phys. Lett. **B390** (1997) 298.

[13] VERMASEREN 1.01 generator: R. Bhattacharya, J. Smith and G. Grammer, Phys. Rev. **D15** (1977) 3267; J. Smith, J.A.M. Vermaseren and G. Grammer, Phys. Rev. **D15** (1977) 3280.

[14] FERMISV generator: J. Hilgart, R. Kleiss and F. Le Diberder, Comp. Phys. Comm. **75** (1993) 191.

[15] OPAL Collaboration, G. Alexander *et al.*, Z. Phys. **C52** (1991) 175.

[16] M. Hauschild *et al.*, Nucl. Inst. and Meth. **A314** (1992) 74.

[17] C. Caso *et al.*, Eur. Phys. J. **C3** (1998) 1.

[18] Y.S. Tsai, Phys. Rev. **D4** (1971) 2821.

[19] W.J. Marciano and A. Sirlin, Phys. Rev. Lett. **61** (1988) 1815.

[20] OPAL Collaboration, G. Alexander *et al.*, Phys. Lett. **B374** (1996) 341.

[21] BES Collaboration, J.Z. Bai *et al.*, Phys. Rev. **D53** (1996) 20.

[22] C.S. Lam and T.M. Yan, Phys. Rev. **D16** (1977) 703.

[23] E. Braaten, Phys. Rev. Lett. **60** (1988) 1606; E. Braaten, Phys. Rev. **D39** (1989) 1458.

[24] E. Braaten, S. Narison and A. Pich, Nucl. Phys. **B373** (1992) 581.

[25] F. Le Diberder and A. Pich, Phys. Lett. **B286** (1992) 147; F. Le Diberder and A. Pich, Phys. Lett. **B289** (1992) 165.

[26] M.A. Shifman, A.I. Vainshtein and V.I. Zakharov, Nucl. Phys. **B147** (1979) 385, 448, 519.

[27] E. Braaten and C.S. Li, Phys. Rev. **D42** (1990) 3888.

[28] A. Pich, **FTUV-97-03** (1997), Invited talk at 20th Johns Hopkins Workshop on Current Problems in Particle Theory, Heidelberg (1996).

[29] S. Narison, Nucl. Phys. **B40** (Proc. Suppl.) (1995) 47.

[30] ALEPH Collaboration, R. Barate *et al.*, Eur. Phys. J. **C4** (1998) 409.

[31] OPAL Collaboration, K. Ackerstaff *et al.*, *Measurement of the Strong Coupling Constant α_s and the Vector and Axial-Vector Spectral Functions in Hadronic Tau Decays*, **CERN-EP/98-102**, (submitted to Eur. Phys. J.).

[32] P.A. Rączka, Phys. Rev. **D57** (1998) 6862.

[33] T. van Ritbergen, J.A.M. Vermaseren and S.A. Larin, Phys. Lett. **B400** (1997) 379.

[34] G. Rodrigo, A. Pich, and A. Santamaria, Phys. Lett. **B424** (1998) 367.

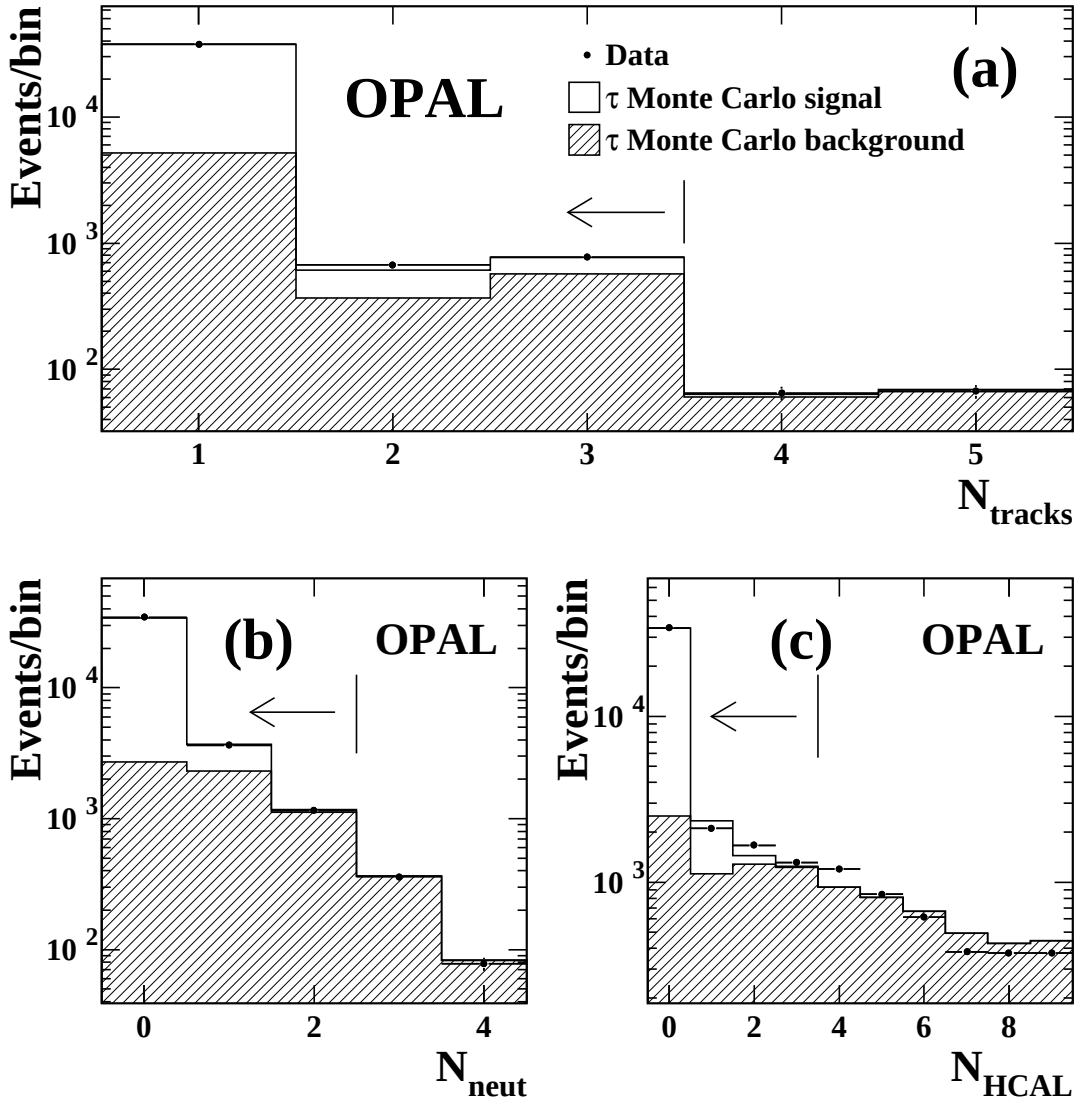

Figure 1: Comparison of data and Monte Carlo simulation of (a) the number of tracks $N_{\rm tracks}$ in the τ jet, (b) the number of neutral clusters $N_{\rm neut}$ and (c) the depth of penetration (in layers) into the HCAL $N_{\rm HCAL}$, for τ jets which have survived all preselection cuts other than the cut on the plotted variable. The selected regions are indicated by the arrows.

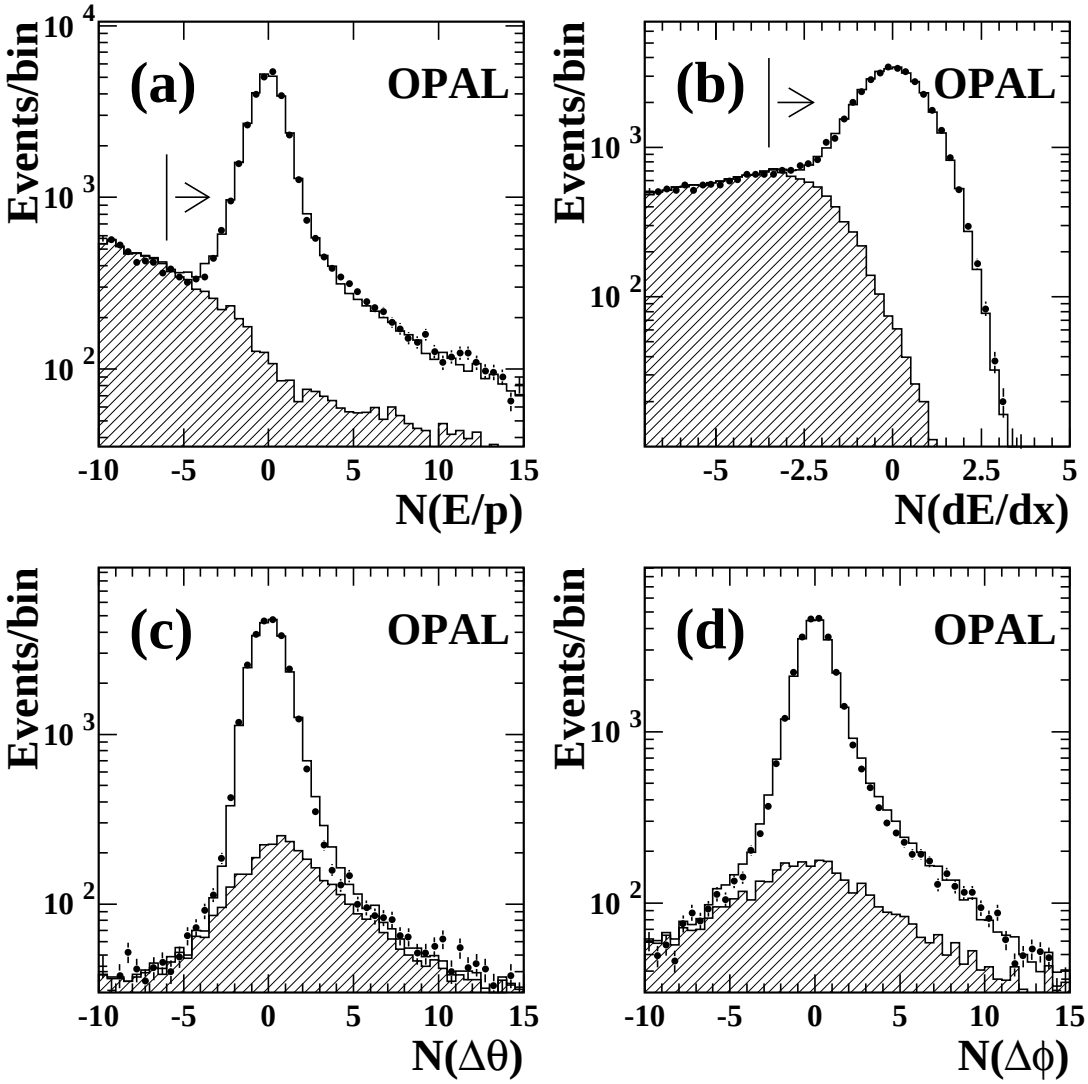

Figure 2: Data and Monte Carlo simulation of the (a) $N(E/p)$ and (b) $N(\mathrm{d}E/\mathrm{d}x)$ distributions for τ jets which have survived all other preselection cuts. The arrows indicate the regions accepted by the preselection cuts. The normalized track-cluster matching variables (c) $N(\Delta\theta)$ and (d) $N(\Delta\phi)$ are shown for all jets which pass the preselection. The points represent data, while the solid and shaded histograms are the τ Monte Carlo signal and background predictions respectively.

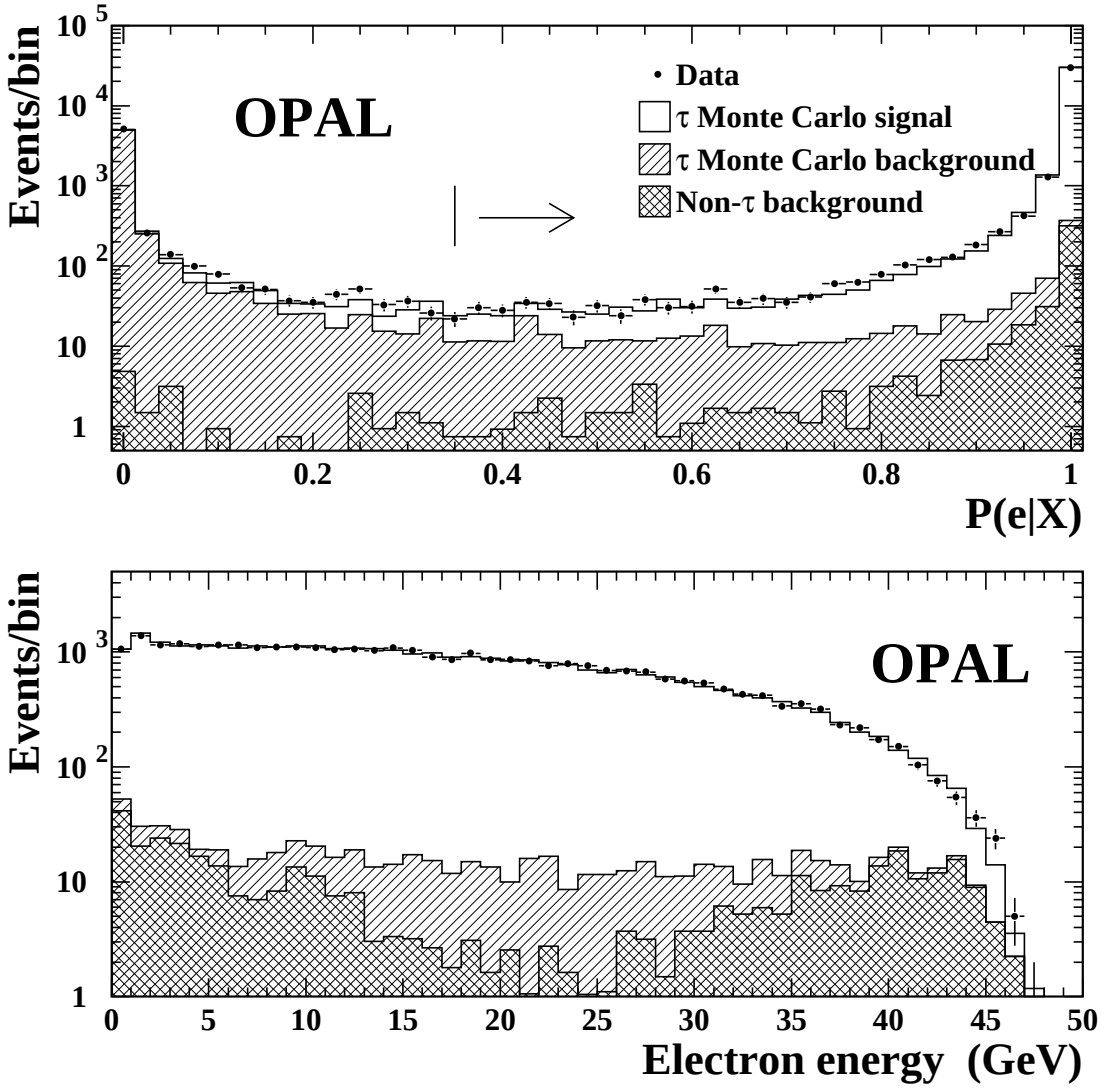

Figure 3: The likelihood selection variable $P(e|X)$ is plotted for all τ jets which pass the preselection (upper plot). The $\tau^- \to \mathrm{e}^-\bar{\nu}_\mathrm{e}\nu_\tau$ candidate sample is composed of all jets in this plot with $P(e|X) > 0.35$ as indicated by the arrow. The energy distribution of jets in the $\tau^- \to \mathrm{e}^-\bar{\nu}_\mathrm{e}\nu_\tau$ candidate sample is shown in the plot below. Monte Carlo predictions for the backgrounds from τ and non-τ sources are indicated.

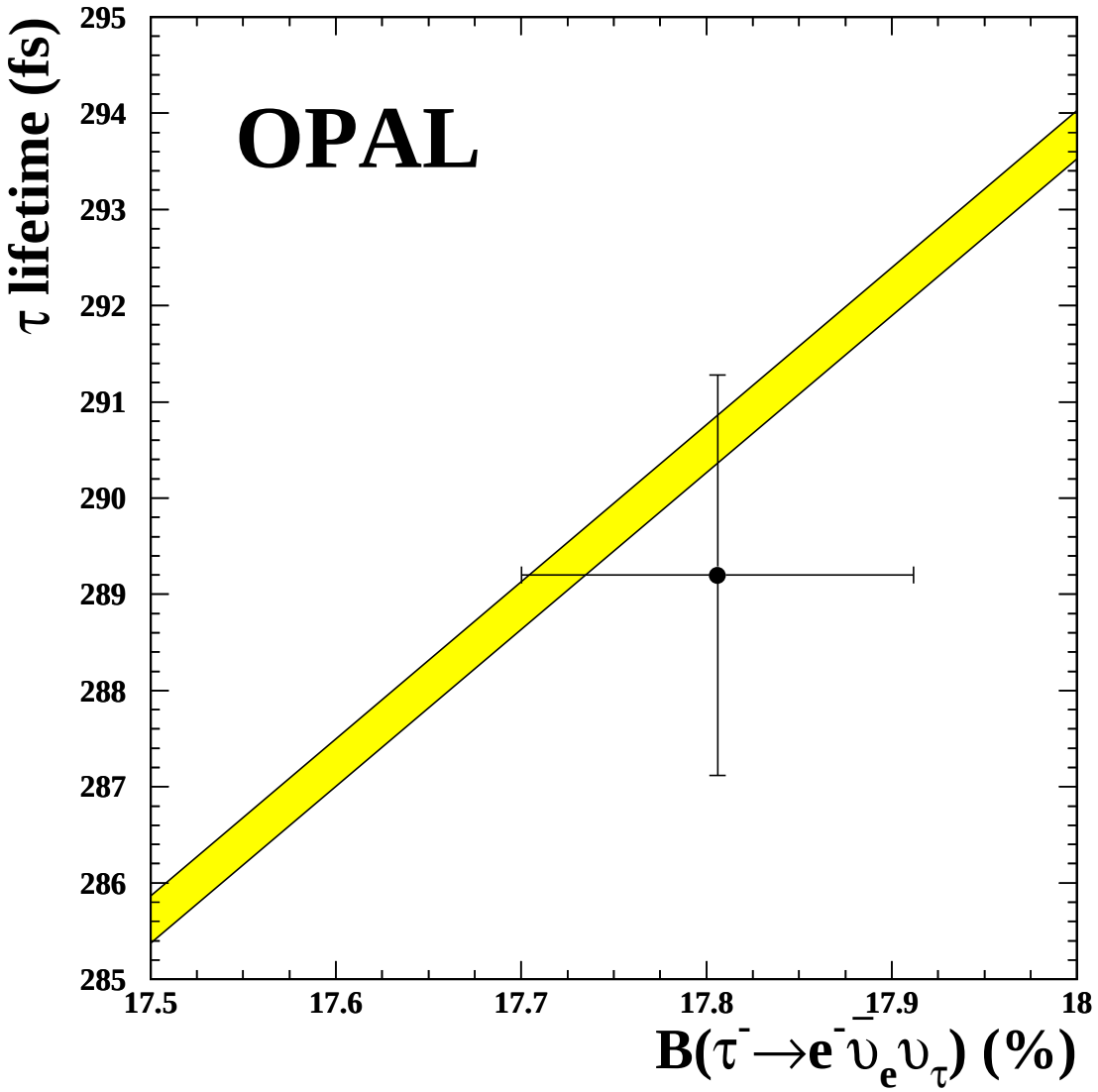

Figure 4: The OPAL τ lifetime is plotted against the $\tau^- \to \mathrm{e}^-\bar{\nu}_\mathrm{e}\nu_\tau$ branching ratio. The shaded band is the Standard Model prediction under the assumption of lepton universality, and its width represents the uncertainty due to the measured τ mass.